Neuron 51, 613–625, September 7, 2006 ©2006 Elsevier Inc. DOI 10.1016/j.neuron.2006.07.024

The Insulin/PI 3-Kinase Pathway Regulates Salt Chemotaxis Learning in *Caenorhabditis elegans*

Masahiro Tomioka,[1,2] Takeshi Adachi,[1,2] Hiroshi Suzuki,[3] Hirofumi Kunitomo,[1] William R. Schafer,[3] and Yuichi Iino[1,*]
[1] Molecular Genetics Research Laboratory
[2] Graduate Program in Biophysics and Biochemistry
Graduate School of Science
The University of Tokyo
7-3-1 Hongo, Bunkyo-ku
Tokyo 113-0033
Japan
[3] Division of Biological Sciences
University of California, San Diego
La Jolla, California 92093

Summary

The insulin-like signaling pathway is known to regulate fat metabolism, dauer formation, and longevity in *Caenorhabditis elegans*. Here, we report that this pathway is also involved in salt chemotaxis learning, in which animals previously exposed to a chemoattractive salt under starvation conditions start to show salt avoidance behavior. Mutants of *ins-1*, *daf-2*, *age-1*, *pdk-1*, and *akt-1*, which encode the homologs of insulin, insulin/IGF-I receptor, PI 3-kinase, phosphoinositide-dependent kinase, and Akt/PKB, respectively, show severe defects in salt chemotaxis learning. *daf-2* and *age-1* act in the ASER salt-sensing neuron, and the activity level of the DAF-2/AGE-1 pathway in this neuron determines the extent and orientation of salt chemotaxis. On the other hand, *ins-1* acts in AIA interneurons, which receive direct synaptic inputs from sensory neurons and also send synaptic outputs to ASER. These results suggest that INS-1 secreted from AIA interneurons provides feedback to ASER to generate plasticity of chemotaxis.

Introduction

Animals show various behaviors in response to environmental stimuli and have abilities to modulate behavior according to past experiences. Behavioral plasticity is caused by changes in the response characteristics of neurons, which are, in many cases, induced by the interplay of multiple neurons in the nervous system. It is therefore important to understand the roles of signaling pathways acting for interneuronal communications underlying behavioral plasticity.

Involvement of the insulin and PI 3-kinase pathways in neural and behavioral plasticity has been highlighted through various observations in mammals. The insulin receptor (IR) is highly expressed in several brain regions, including the hippocampus and cerebellum, and its inhibition in the central nervous system causes deficits in learning and memory (Zhao et al., 2004). In hippocampal CA1 neurons, insulin causes long-term depression of synaptic transmission by decreasing AMPA receptors on the plasma membrane (Man et al., 2000). The PI 3-kinase pathway is one of the signaling pathways acting downstream of receptor and nonreceptor tyrosine kinases, including the insulin receptor. Its importance for neuronal plasticity has been demonstrated by impaired amygdala LTP in rats after pharmacological inhibition of PI 3-kinase (Lin et al., 2001). Inhibition of PI 3-kinase also impairs synaptic insertion of AMPA receptors during hippocampal LTP (Man et al., 2003). In spite of these observations, the understanding of the role of the insulin/PI 3-kinase signaling pathway in synaptic and behavioral plasticity is fragmentary, and the significance of this pathway is unclear.

To assess the importance of signaling pathways in behavioral plasticity and understand how they act, a simple model organism such as *Caenorhabditis elegans* is beneficial. The nervous system of *C. elegans* is composed of 302 neurons, and their neural connections are fully described (White et al., 1986). Worms sense volatile and water-soluble chemicals by sensory neurons in the head and tail and show chemotaxis to these chemicals. This chemotaxis behavior shows several forms of plasticity (Hobert, 2003). For example, prolonged exposure to attractive odorants leads to a reduction of chemotaxis to these odorants in a process called "olfactory adaptation" (Colbert and Bargmann, 1995). Several molecules, including OSM-9, a TRP-like ion channel (Colbert and Bargmann, 1995; Colbert et al., 1997), EGL-4, a cGMP-dependent protein kinase (L'Etoile et al., 2002), and ADP-1, whose molecular identity is unknown (Colbert and Bargmann, 1995), are essential for olfactory adaptation. In another form of plasticity, worms subjected to prolonged exposure to attractive salts, such as NaCl, under starvation conditions show a dramatic reduction of chemotaxis to salts and eventually show a negative chemotaxis. Exposure to salts in the presence of food does not lead to a reduction of chemotaxis, suggesting that worms change their behavior by integrating two stimuli, salt and starvation (Saeki et al., 2001). HEN-1, a secretory protein with an LDL receptor motif that is expressed in two types of neurons, ASE salt-sensing neurons and AIY interneurons, is involved in this type of learning as well as other integrative sensory processing (Ishihara et al., 2002). Mutants affected in G protein signaling, Ca^{2+} signaling, and cGMP signaling show defects in a similar assay for plasticity of salt chemotaxis (Hukema et al., 2006).

The insulin-like signaling pathway in this organism is known to regulate dauer larva formation, an alternative developmental program that occurs under starvation and overcrowding in wild-type animals (Paradis et al., 1999). The components of the insulin-like signaling pathway are highly conserved with those in mammals, including DAF-2, a homolog of the insulin/IGF-I receptor, AGE-1, a PI 3-kinase homolog, DAF-18, a PTEN homolog, PDK-1 and AKT-1/2, homologs of phosphoinositide-dependent protein kinases, and DAF-16, a FOXO family transcription factor (Paradis et al., 1999). Apart from dauer larva formation, the pathway is also involved

*Correspondence: iino@gen.s.u-tokyo.ac.jp

in the control of longevity, fat accumulation, sensitivity to hypoxia, and thermotaxis (Murakami et al., 2005; Paradis et al., 1999; Scott et al., 2002).

Here we present evidence that the insulin-like signaling pathway regulates behavioral plasticity in *C. elegans*. Mutants affected in the insulin-like signaling pathway show severe defects in the behavioral plasticity induced by prolonged exposure to salt. A balance between the PI 3-kinase AGE-1 and the PTEN phosphatase DAF-18 regulates the extent and orientation of salt chemotaxis in the ASER sensory neuron. On the other hand, the insulin-like molecule INS-1 acts in AIA interneurons that receive direct synaptic input from sensory neurons and also send synaptic outputs to ASER. These observations reveal the importance of the feedback regulation by the insulin/PI 3-kinase pathway in behavioral plasticity in *C. elegans*.

Results

Identification of *daf-2* as Learning-Defective Mutants

We have previously reported that *C. elegans* learns to avoid NaCl after being exposed to NaCl under starvation conditions (Saeki et al., 2001). In this study, a simplified version of the assay was employed (Figure 1A). After soaking in a NaCl-containing buffer for 1 hr (NaCl conditioning), worms show negative chemotaxis to NaCl (Figures 1B and 1C and see Movies S1 and S2 in the Supplemental Data available online). However, treatment with a buffer without NaCl (mock conditioning) does not cause this dramatic change of chemotaxis to the opposite direction (Figure 1B and Movie S3) but causes an increase in chemotaxis. This improvement of chemotaxis by buffer treatment is not the subject of this study but will be briefly discussed in the Discussion. As reported previously (Saeki et al., 2001), no decrease in chemotaxis is observed when worms are exposed to NaCl in the presence of food (Figure S1A). Chemotaxis to odorants does not significantly change by conditioning with NaCl, indicating that the behavioral change is not caused by nonspecific effects of salt treatment (Figure 1B and Figure S1A). Chemotaxis to NaCl is dramatically decreased after soaking in a NaCl-containing buffer for 10 min and then is gradually decreased further after a longer conditioning (Figure 1C). The time course of the change in chemotaxis resembles that of a similar salt-plasticity assay reported by Jansen et al. (Jansen et al., 2002). NaCl-conditioned animals keep avoiding NaCl for about half an hour, suggesting formation of a stable memory (Figure 1D). For simplicity, we hereafter call this form of behavioral plasticity "salt chemotaxis learning."

To gain insights into the molecular mechanisms of salt chemotaxis learning, we searched for learning-defective mutants through existing mutants affected in the regulatory functions of the nervous system. We focused on dauer larva formation (*daf*) mutants because many *daf* genes act in neurons to regulate dauer larva formation in response to environmental cues and might also be involved in other aspects of neuronal control (Riddle and Albert, 1997). Among the *daf* mutants tested, we found that the *daf-2* mutants showed a strong defect in salt chemotaxis learning. *daf-2* mutants showed normal chemotaxis to NaCl after mock conditioning but showed only a small decrease of chemotaxis after exposure to NaCl (Figure 1E and Figure S1B). Water-soluble chemicals including NaCl are mainly sensed by ASE neurons (Bargmann and Mori, 1997). As reported previously (Saeki et al., 2001), NaCl conditioning also decreases chemotaxis to several ASE-sensed chemicals, such as cAMP, biotin, and lysine (Figure S2). *daf-2* mutants also showed a defect in the plasticity of chemotaxis to these ASE-sensed chemicals (Figure S2).

daf-2(e1370) mutants are temperature sensitive: they show a dauer-constitutive phenotype and therefore fail to grow to adults at temperatures above 20°C, while they grow normally at 15°C (Kimura et al., 1997). The learning defect was observed when *daf-2(e1370)* mutants were grown at 15°C and conditioned and tested at 25°C. In contrast, the learning defect was not observed at 15°C (Figure 1F). Several different alleles of *daf-2* also showed defects in learning (Figure S3).

Components of the Insulin-like Signaling Pathway Are Required for Salt Chemotaxis Learning

daf-2 encodes the only *C. elegans* homolog of insulin and IGF-I receptors (Kimura et al., 1997). Previous studies on the dauer formation and longevity pathways have revealed several genes that act in this pathway, all of which encode phylogenetically conserved proteins. We therefore asked which of these genes are also involved in salt chemotaxis learning. Genes that act downstream of *daf-2* include *age-1*, which encodes a homolog of the catalytic subunit of PI 3-kinase thought to be coupled to the DAF-2 receptor; *pdk-1*, which encodes a phosphoinositide-dependent protein kinase homolog; and *akt-1* and *akt-2*, which encode Akt/PKB homologs (Paradis et al., 1999). Both PDK and Akt/PKB kinases are activated by 3-phosphoinositides, the product of PI 3-kinase. Of these, loss-of-function mutants of *age-1*, *pdk-1*, and *akt-1* showed defects in the salt learning assay, which were similar to *daf-2* mutants (Figures 2A and 2B). These results suggest that the kinase cascade of PDK and Akt/PKB is required downstream of DAF-2 receptor and AGE-1 PI 3-kinase for salt chemotaxis learning.

Lack of DAF-18 PTEN Causes a Decrease of Chemotaxis

Given that impairment of the DAF-2/AGE-1 signaling causes learning defects, it is of interest to see the consequence of hyperactivation of this signal. *daf-18* encodes a homolog of PTEN phosphatase, which catalyzes dephosphorylation of 3-phosphoinositides such as $PI(3,4,5)P_3$, the reverse reaction of PI 3-kinase (Solari et al., 2005). Therefore, the 3-phosphoinositide level is raised in *daf-18* mutants, and they show a dauer-defective phenotype, which is opposite to *age-1* and *daf-2* mutants (Solari et al., 2005). We found that both the reduction-of-function and null mutants of *daf-18*, *daf-18(e1375)*, and *daf-18(mg198)*, respectively, showed negative or reduced chemotaxis to NaCl both in naive animals and after treatment in a NaCl-free buffer (Figures 2A and 2B, hatched or open bars). The phenotype implies that 3-phosphoinositides may negatively regulate salt chemotaxis. To further dissect the effect of the *daf-18* mutations, we tested the phenotypes of double mutants. *daf-2(e1370)*, *daf-2(sa189)*, *age-1(hx546)*,

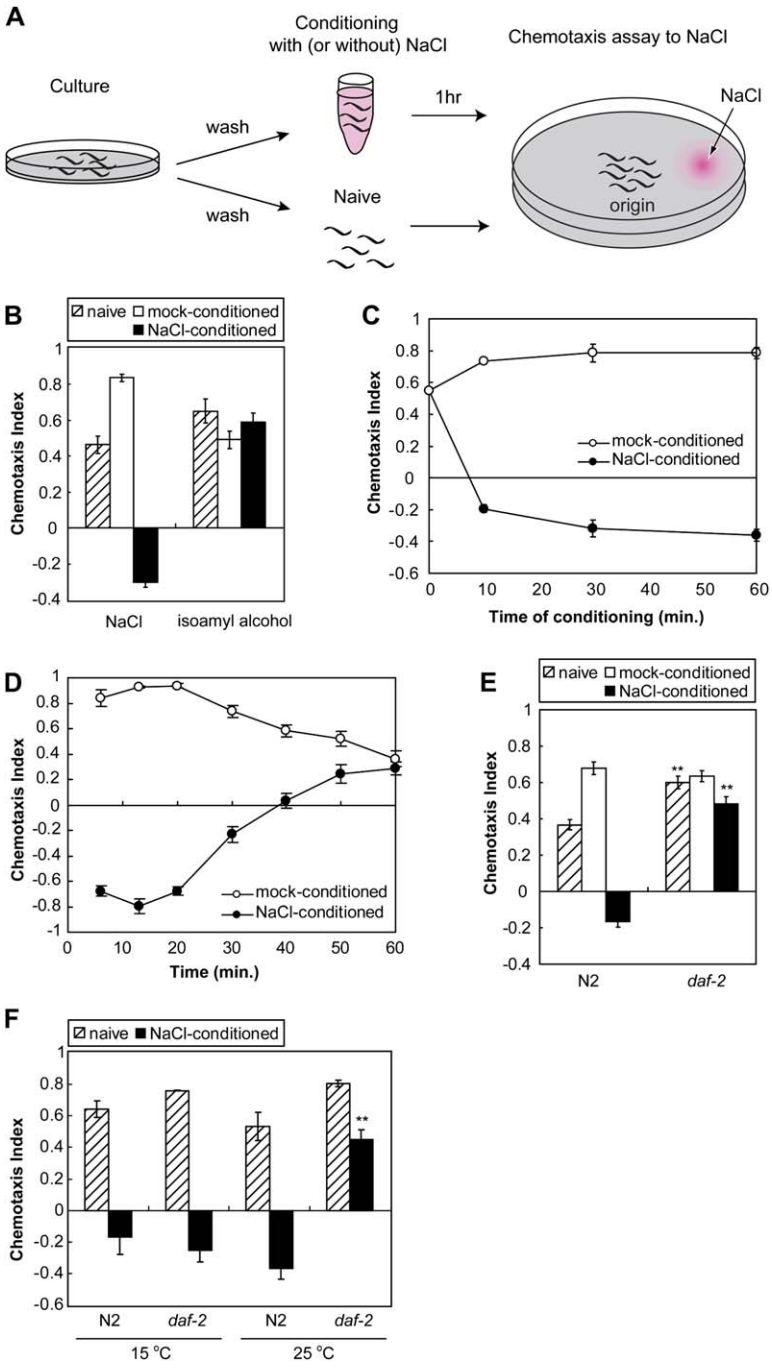

Figure 1. Salt Chemotaxis Learning Is Impaired in *daf-2* Mutants

(A) Procedures for the salt chemotaxis learning assay. Worms are collected from the culture plate, treated in a buffer with or without NaCl, and chemotaxsis to NaCl is tested.

(B) Salt chemotaxis learning in wild-type N2 animals. Chemotaxis to 100 mM NaCl (left) and 10^{-4} dilution of isoamyl alcohol (right) after pretreatment in a buffer with NaCl ("NaCl conditioned") or without NaCl ("mock conditioned") for 1 hr is shown for the wild-type strain. Negative chemotaxis is observed only after conditioning with NaCl. "Naive" indicates chemotaxis of animals without any prior treatment.

(C) Time course of the induction of the behavioral plasticity of NaCl chemotaxis. Wild-type N2 animals were treated in a NaCl-containing buffer or NaCl-free buffer for various durations and tested for chemotaxis to NaCl.

(D) Time course of recovery from conditioned state. Wild-type N2 animals were conditioned, and chemotaxis to NaCl was tested. Chemotaxis index is shown for various time points after animals were placed on chemotaxis plates. The detailed procedure can be seen in the Supplemental Data available online.

(E) Learning defect of *daf-2* mutants. Wild-type N2 and *daf-2(e1370)* mutants were conditioned, and chemotaxis to NaCl was tested.

(F) The learning defect of *daf-2(e1370)* mutants is temperature sensitive. *daf-2(e1370)* mutants were grown at 15°C and conditioned and tested either at 25°C or 15°C as indicated. Double asterisks represent significant differences from wild-type N2 (**$p < 0.001$ by Student's t test).

Error bars represent SEM.

and *akt-1(ok525)* mutations partially or fully suppressed the reduced chemotaxis of *daf-18(e1375)* in double mutants, suggesting that hyperactivation of the DAF-2/AGE-1 pathway caused the reduction of chemotaxis in *daf-18* mutants as expected (Figures 2A and 2B, hatched or open bars). Chemotaxis after salt conditioning was similarly affected by these mutations. Introduction of the *daf-18(e1375)* mutation dramatically reduced the chemotaxis of salt-conditioned *daf-2(e1370)*, *daf-2(sa189)*, and *age-1(hx546)* mutants to negative values. On the other hand, chemotaxis of the strong mutant of *age-1*, *age-1(mg305)*, was hardly affected by *daf-18* (Figures 2A and 2B, filled bars). These results suggest that residual activity of DAF-2 or AGE-1 carrying weak reduction-of-function mutations can be augmented by lack of DAF-18 PTEN and that extent and orientation of chemotaxis is very sensitive to phosphoinositide levels. Although the null mutants of *daf-2* and *age-1* are lethal, the lethality of the *age-1(m333)* null mutant can be rescued by the *daf-18* mutations. In the *age-1(m333); daf-18(mg198)* double null mutants, only a small extent of salt chemotaxis learning occurred, indicating that the AGE-1 pathway plays a major role for salt chemotaxis learning compared to other signaling pathways known to be involved in the behavioral plasticity (Figure 2A and Figure S4).

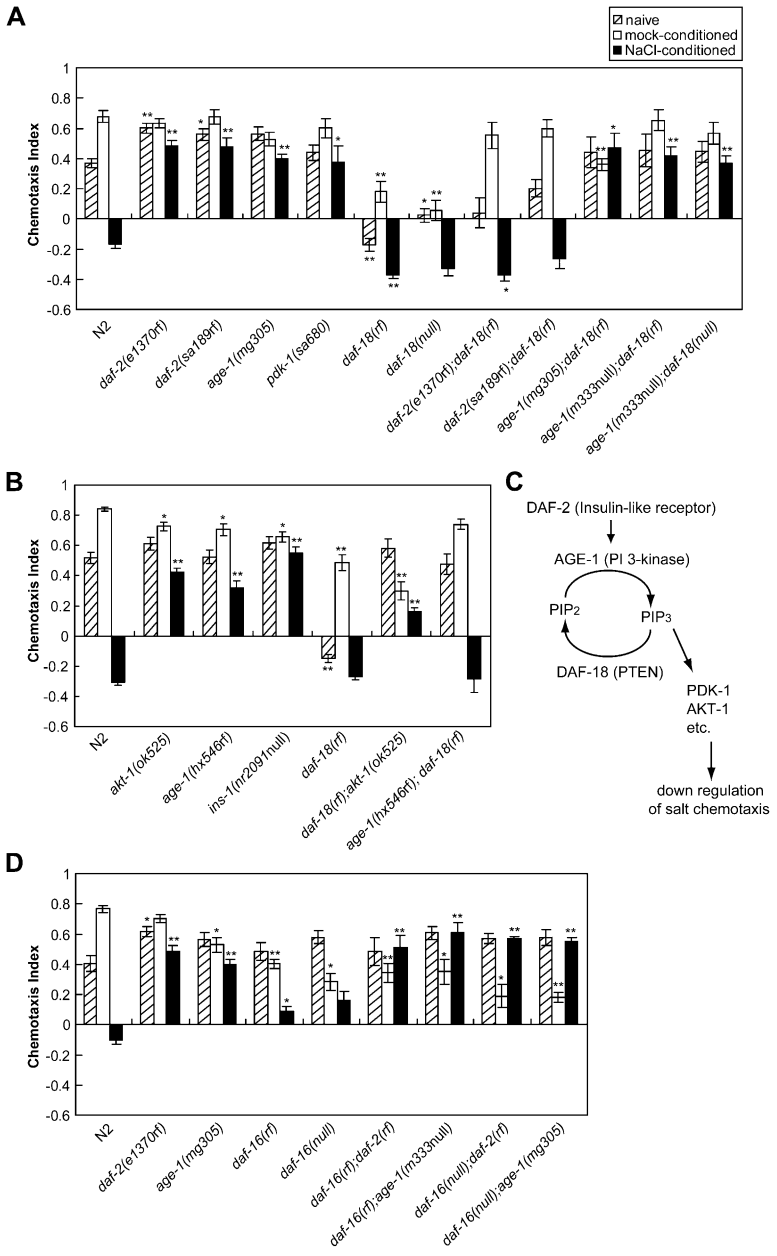

Figure 2. Salt Chemotaxis Learning Is Impaired in Mutants of the Insulin-like Signaling Pathway

(A) The following strains were grown at 15°C, and salt chemotaxis learning assay was performed: wild-type N2, *daf-2(e1370rf)*, *daf-2(sa189rf)*, *age-1(mg305)*, *pdk-1(sa680)*, *daf-18(e1375rf)*, *daf-18(mg198null)*, *daf-2(e1370rf); daf-18(e1375rf)*, *daf-2(sa189rf); daf-18(e1375rf)*, *age-1(mg305); daf-18(e1375rf)*, *age-1(m333null); daf-18(e1375rf)*, and *age-1(m333null); daf-18(mg198null)*.

(B) The following strains were grown at 20°C, and salt chemotaxis learning assay was performed: wild-type N2, *akt-1(ok525)*, *age-1(hx546rf)*, *ins-1(nr2091null)*, *daf-18(e1375rf)*, *daf-18(e1375rf); akt-1(ok525)*, and *age-1(hx546rf); daf-18(e1375rf)*.

(C) A model for the regulation of salt chemotaxis learning by the insulin-like signaling pathway.

(D) The following strains were grown at 15°C, and salt chemotaxis learning assay was performed: wild-type N2, *daf-2(e1370rf)*, *age-1(mg305)*, *daf-16(m26rf)*, *daf-16(mgDf47null)*, *daf-16(m26rf); daf-2(e1370rf)*, *daf-16(m26rf); age-1(m333null)*, *daf-16(mgDf47null); daf-2(e1370rf)*, and *daf-16(mgDf47null); age-1(mg305)*. Asterisks represent significant differences from wild-type N2 (*$p < 0.01$, **$p < 0.001$ by Student's t test).

Error bars represent SEM.

INS-1 Insulin Is Required for Salt Chemotaxis Learning

The insulin-like peptide DAF-28 is required for dauer formation (Li et al., 2003). However, *daf-28* mutants were normal in our salt learning assay (data not shown). In addition to *daf-28*, 37 insulin-like genes have been predicted in the *C. elegans* genome. We therefore tested available mutants of the insulin-like genes, including *ins-1*, whose predicted product is the most similar to human insulin (Pierce et al., 2001). We found that the deletion mutant of *ins-1*, *ins-1(nr2091)*, showed a clear defect in salt chemotaxis learning (Figure 2B), while it was normal in dauer formation and had a wild-type lifespan (Pierce et al., 2001). These data suggest that different insulin-like peptides are used for different biological processes; DAF-28 mainly acts for dauer formation and INS-1 mainly for salt chemotaxis learning.

We also tested the FOXO family transcription factor DAF-16, which is known to act for both dauer and longevity controls (Paradis et al., 1999). Mock-conditioned *daf-16(m26)* reduction-of-function and *daf-16(mgDf47)* null mutants showed reduced chemotaxis (Figure 2D), which suggested that it might be somehow involved in the regulation of chemotaxis. In dauer and longevity controls, DAF-16 is negatively regulated by the DAF-2/AGE-1 pathway; *daf-16* mutations suppress the dauer-constitutive and long-life phenotypes of *daf-2* and *age-1* mutants (Paradis et al., 1999). It also suppresses the enhanced thermotaxis of *daf-2* and *age-1* mutants (Murakami et al., 2005). However, *daf-16* mutants did not suppress *daf-2* and *age-1* mutants in salt chemotaxis learning (Figure 2D). In addition, the phenotypes of *daf-16* single mutants and double mutants *daf-16; daf-2* or *daf-16; age-1* were largely different. Therefore,

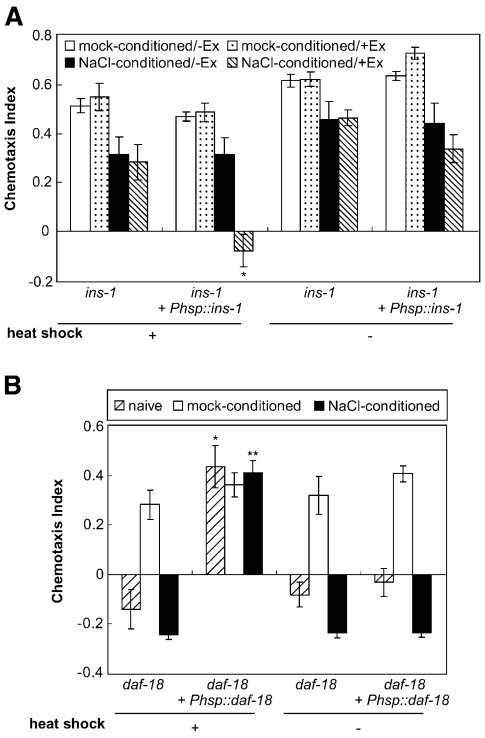

Figure 3. *ins-1* and *daf-18* Act at the Adult Stage in Salt Chemotaxis Learning

(A) Learning defect is rescued in *ins-1(nr2091)* animals carrying *Phsp::ins-1* after heat shock at the adult stage. "+Ex" indicates animals carrying the transgene, and "−Ex" indicates animals not carrying the transgene. (B) Defect of NaCl chemotaxis is rescued in *daf-18(e1375)* animals carrying *Phsp::daf-18* after heat shock at the adult stage. In (A) and (B), control animals carry only a transformation marker (*Pmyo-3::gfp*). Asterisks represent significant difference from both the control animals without heat shock and without transgene (*$p < 0.01$, **$p < 0.001$ by Student's t test). Error bars represent SEM.

although DAF-16 might act downstream of the DAF-2/AGE-1 pathway, it cannot be the sole downstream target of the pathway, and factors other than DAF-16 should act for salt chemotaxis learning.

The Insulin-like Pathway Acts at the Postdevelopmental Stage

The insulin-like signaling pathway could either affect development or act in the mature neural circuit to regulate salt chemotaxis learning. We tested these possibilities by heat-shock rescue experiments. Development of the nervous system occurs mostly in embryos; a subset of neurons is generated and mature during early larval stages in *C. elegans*. INS-1 was expressed from a transgene in the *ins-1(nr2091)* mutants under the control of the heat-shock promoter *Phsp16-2*. When heat shock was applied at the adult stage, the learning defect was rescued in the *ins-1* mutants carrying the transgene (Figure 3A). This result indicates that the action of *ins-1* at the adult stage is sufficient for salt chemotaxis learning. When *daf-18* was similarly expressed at the adult stage using the heat-shock promoter, the chemotaxis defect in the *daf-18(e1375)* mutants was rescued (Figure 3B, hatched bars), suggesting that the action of *daf-18* at the adult stage is sufficient for normal chemotaxis to NaCl and that the chemotaxis defect of *daf-18* mutants is unlikely to be due to developmental defects. In addition, salt chemotaxis learning was inhibited in animals where *daf-18* expression was induced (Figure 3B, filled bars). We speculate that the overproduction of DAF-18 caused a decrease of the intracellular level of 3-phosphoinositides, which led to a learning defect similar to *age-1* mutants.

AGE-1 Acts in the Right Salt-Sensing Neuron, ASER

To examine where in the neural circuit the insulin-like signaling pathway acts to alter chemotaxis behavior, we expressed *age-1* cDNA in various neurons in *age-1(hx546)* mutants using cell-specific promoters and examined which promoter-driven cDNA rescued the learning defect in the mutants. When *age-1* was expressed using the *gcy-5* and *gcy-7* promoters or the *ceh-36* promoter in ASE neurons, the main salt-sensing chemosensory neurons, the learning defect was rescued, while it was not rescued by expression in the salt-sensing chemosensory neurons other than ASE or in several interneurons (Figures 4A and 4C). These data suggest that *age-1* mainly acts in ASE neurons. These neurons consist of a pair of neurons, ASEL and ASER, which are bilaterally symmetrical in morphology. When *age-1* was only expressed in ASER neurons using the *gcy-5* promoter, learning defects of the *age-1(hx546)* mutants were completely rescued, while they were not rescued by expression in ASEL neurons using the *gcy-7* or *lim-6* promoter (Figure 4A). This indicates that *age-1* acts only in the ASER neuron. Expression of *daf-2* in ASER neurons partially rescued the learning defect of the *daf-2(e1370)* mutants, while expression in ASEL neurons did not (Figure S5), suggesting that *daf-2* also acts in the ASER neuron. The rescue was weak possibly due to the difficulty to express DAF-2 protein from the cDNA. However, it does not rule out the possible role of *daf-2* in neurons other than ASE.

DAF-18 PTEN Is Localized to the Surface of the Cell Body and Neurites, but Not to the Sensory Cilia of ASER

Reduced chemotaxis to NaCl of *daf-18* mutants was rescued by the expression of *daf-18* in ASER neurons, but not in ASEL neurons, suggesting that DAF-18 PTEN also acts in ASER neurons for efficient chemotaxis (Figure 4B). To gain insights into the role of DAF-18 PTEN in ASER, we observed the localization of the DAF-18 protein that was fused with Venus, a modified green fluorescent protein (Nagai et al., 2002), and expressed in ASER neurons. Functional DAF-18::Venus was localized to the surface of the cell body, dendrite, and axon, but not to the cilia (Figure S6), suggesting that DAF-18 is likely to act at a site other than the cilia, where sensory signal transduction occurs.

We also attempted to determine the intracellular localization of AGE-1 and DAF-2 in ASER neurons using fusion proteins with GFP or Venus. AGE-1::GFP was observed throughout the cell, while expression of DAF-2::Venus was too weak to determine the precise localization (data not shown).

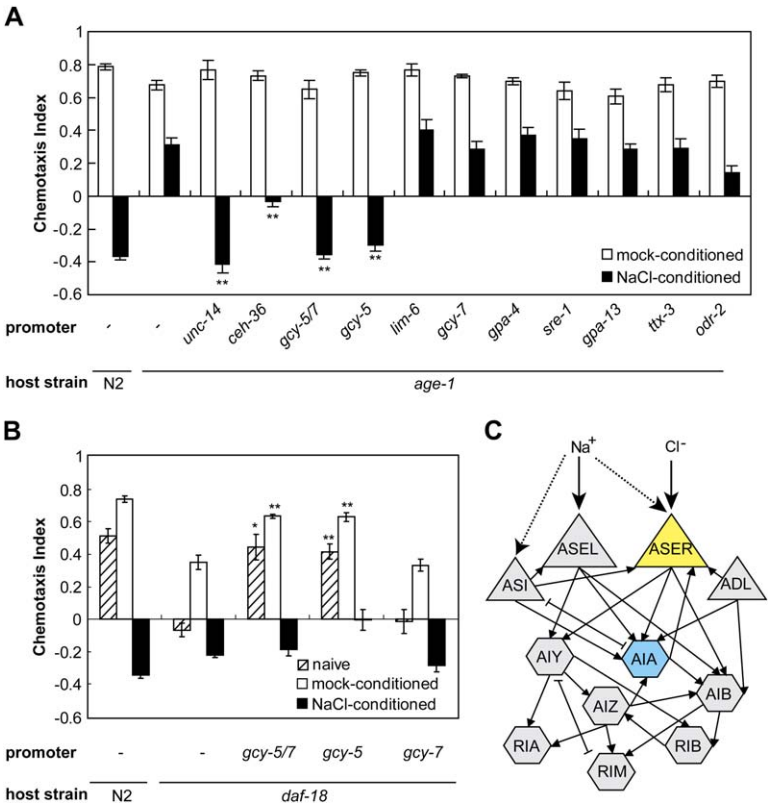

Figure 4. *age-1* and *daf-18* Act in the ASER Neuron for Salt Chemotaxis Learning

(A) The learning defect of *age-1(hx546)* animals is rescued by the expression of *age-1* in all neurons using the *unc-14* promoter, in the ASER/L neurons using *ceh-36* or *gcy-5* and *gcy-7* promoters, or in ASER neurons using the *gcy-5* promoter alone. On the other hand, it is not rescued by the expression in ASEL neurons using the *lim-6* or *gcy-7* promoter, in ASI neurons using the *gpa-4* promoter, in ADL and ASJ neurons using the *sre-1* promoter, in several neurons including ASH and ADF using the *gpa-13* promoter, in AIY neurons using the *ttx-3* promoter, or in several neurons including ASG and AIZ using the *odr-2* promoter. (B) The NaCl chemotaxis defects of *daf-18(e1375)* animals both in naive conditions and after mock conditioning are rescued by the expression of *daf-18* in ASER neurons using the *gcy-5* promoter, but it is not rescued by the expression in ASEL neurons using the *gcy-7* promoter. In (A) and (B), asterisks represent significant differences from control animals carrying only the transformation marker (*$p < 0.01$, **$p < 0.001$ by Student's t test). (C) Part of the neural circuit for salt chemotaxis (White et al., 1986). Na^+ ions are sensed mainly by ASEL sensory neurons and weakly in ASER and other sensory neurons such as ASI. Cl^- ions are sensed mainly by ASER sensory neurons (Bargmann and Mori, 1997; Pierce-Shimomura et al., 2001). Arrows indicate synaptic connections, and H shapes indicate gap junctions. Triangles and hexagons represent sensory neurons and interneurons, respectively. Error bars represent SEM.

Sensory Response of ASER Neurons Is Intact in *daf-18* and Other Mutants of the Insulin-like Pathway

To further characterize the nature of the chemotaxis defect of *daf-18* mutants, we monitored the sensory response of ASER neurons by following the activation of MAP kinase (MAPK). MAPK was previously shown to be activated in olfactory neurons upon odorant stimulus, which was probably dependent on membrane depolarization because the activation did not occur in mutants of cyclic nucleotide-gated channel or voltage-gated calcium channel (Hirotsu et al., 2000). In ASER neurons, MAPK was activated within 1 min of removal of NaCl (Figures 5A–5C). This off-response was expected because worms respond to reduction of salt concentrations and change their direction of movement (Faumont et al., 2005; Miller et al., 2005; Pierce-Shimomura et al., 2001). The off-response of MAPK was similarly observed in naive animals and animals conditioned in NaCl for 60 min (data not shown). The same pattern of activation was observed in *daf-18(mg198)* mutants as well as *daf-2(e1370)*, *age-1(hx546)*, and *ins-1(nr2091)* mutants (Figure 5D).

We also monitored the activity of ASER neurons by in vivo calcium imaging using a genetically encoded calcium sensor, cameleon (Hilliard et al., 2005; Suzuki et al., 2003). Similar to the activation of MAPK, fast calcium transients, which presumably reflect depolarization of the ASER neuron, were observed upon NaCl downshift (Figure 5E). Detailed analyses of calcium response in ASE neurons will be published elsewhere (H.S. and W.R.S., unpublished data). The calcium response was not significantly affected by NaCl conditioning (data not shown). *daf-18(mg198)* and *age-1(hx546)* also showed steep calcium transients upon NaCl downshift, and the response magnitude was comparable to the wild-type animals (Figures 5E and 5F).

These results support the view that the chemotaxis defect of *daf-18* mutants and the learning defects of *daf-2*, *age-1*, and *ins-1* mutants are not caused by sensory defects of the ASER neuron; they further suggest that salt chemotaxis learning and the insulin-like pathway regulate intracellular processes that occur after excitation of the sensory neuron, such as synaptic output.

INS-1 Insulin Is Localized to the Synaptic Regions of AIA Interneurons

We have so far shown evidence that the DAF-2/AGE-1 pathway acts in the ASER sensory neuron. Where, then, does the insulin-like peptide INS-1 act? To answer this question, we first observed the expression of the INS-1 protein fused with Venus. INS-1::Venus, which we confirmed to be functional (Figure 6H), was expressed in several amphid chemosensory neurons, ASE, ASI, and ASJ; AIA interneurons; and several other neurons. Of these expression patterns, the fluorescence signal in AIA was the strongest and most consistent between individual animals (Figures 6A–6C and data not shown). AIA are interneurons that receive synaptic

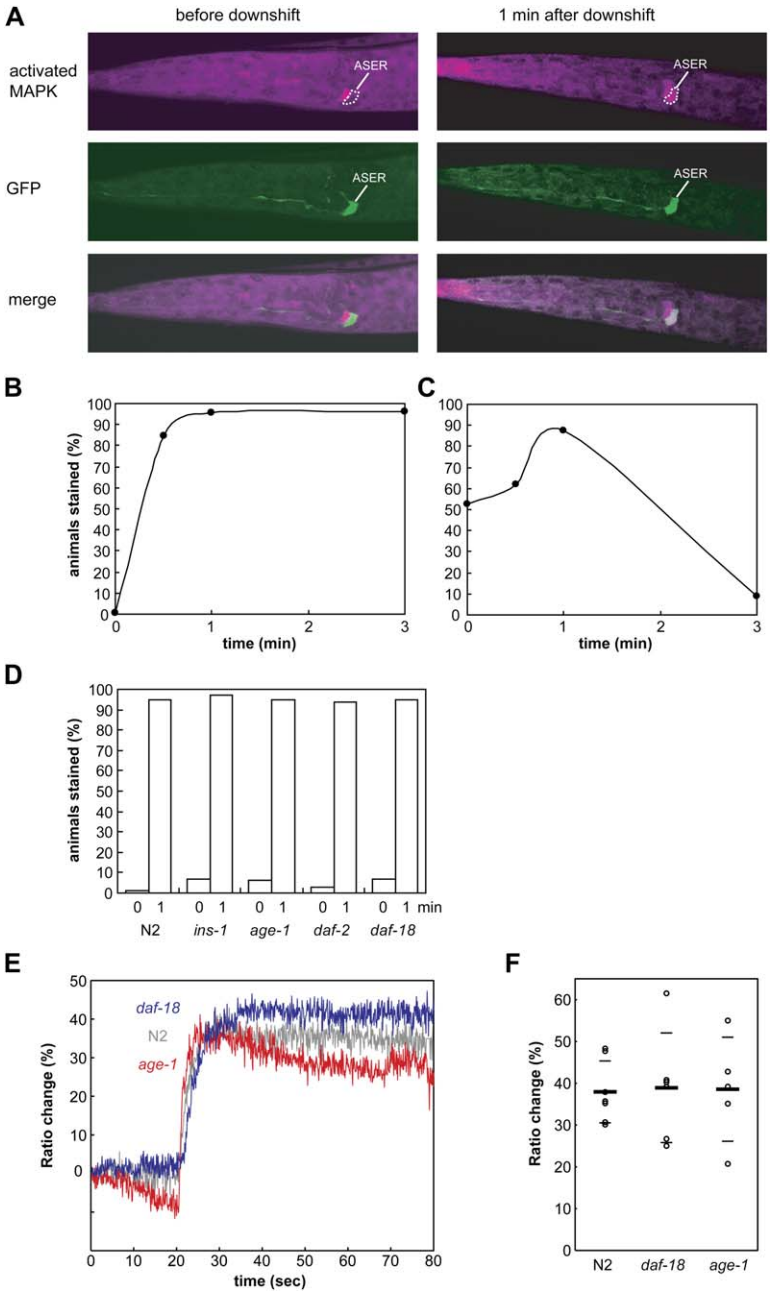

Figure 5. Sensory Response of ASER Neurons Is Intact in Mutants of the Insulin-like Pathway

(A) A strain expressing GFP in ASER neurons from the *Pgcy-5::gfp* transgene (*ntIs1*; Chang et al., 2003) was subjected to immunohistochemistry before and 1 min after downshift of NaCl concentration from 50 mM to 0 mM. Activation of MAP kinase was observed using the anti-activated-MAPK antibody, while ASER was identified by the anti-GFP antibodies. Note that MAPK is constitutively activated in an unidentified neuron located just anterior to ASER.

(B) Time course of MAPK activation. Animals carrying the *Pgcy-5::gfp* transgene were washed from culture plates, kept in a buffer containing 50 mM NaCl for 10 min, and transferred to a NaCl-free buffer. Fraction of animals in which ASER was stained for activated MAPK is shown at intervals after the NaCl downstep.

(C) Time course of MAPK inactivation. Animals were collected, kept in a NaCl-free buffer for 10 min, and transferred to a buffer containing 50 mM NaCl. Fraction of activated MAPK after the NaCl upstep is shown at intervals.

(D) MAPK response in mutants. MAPK activation was observed as in (B) in each mutant carrying the *Pgcy-5::gfp* transgene before and 1 min after the NaCl downstep. Mutants used were *ins-1(nr2091*null*)*, *age-1(hx546*rf*)*, *daf-2(e1370*rf*)*, and *daf-18(mg198*null*)*.

(E) Calcium transients in ASER induced by 40–0 mM NaCl downstep. ASER neuronal response was observed by in vivo calcium imaging from strains expressing YC2.12 in ASE neurons (see Experimental Procedures). Worms were exposed to a constant flow of saline containing 40 mM NaCl for ~20 min before imaging. At 20 s in imaging, the worm's head was covered by a stream of stimulant saline containing 0 mM NaCl to apply 40–0 mM NaCl downstep stimulation. Neuronal response of ASER was expressed as the change of YFP/CFP ratio.

(F) Comparison of ASER response magnitude. The ratio increase was quantified and plotted for N2 wild-type (n = 7), *daf-18(mg198*null*)* (n = 6), and *age-1(hx546*rf*)* (n = 5). Each circle shows ASER response from a different worm and horizontal bars for mean ± standard deviation. Significant difference between wild-type and either of the mutants was not detected by Mann-Whitney statistic test (p = 0.943 for N2 versus *daf-18*, and p = 0.817 for N2 versus *age-1*).

inputs from several classes of sensory neurons including ASE and also send synaptic outputs to ASER at the contacts between their processes that run side by side in the nerve ring (White et al., 1986). In AIA neurons, punctate expression patterns in the cell bodies and processes were observed (Figure 6C). In *unc-104* mutants, INS-1::Venus was diminished from the processes in the nerve ring and concentrated in the cell bodies (Figure 6D). The *unc-104* gene encodes a KIF1-like kinesin required for efficient transport of synaptic vesicles and dense-core vesicles to neuronal processes, and mutants of this gene accumulate synaptic vesicle and dense-core vesicle proteins in cell bodies (Nonet et al., 1998; Zahn et al., 2004). Next, we examined the localization of INS-1::Venus relative to the synaptic vesicle protein SNB-1 synaptobrevin fused with mRFP in nerve ring processes (Nonet et al., 1998). INS-1::Venus and SNB-1::mRFP were colocalized in the processes of *ins-1*-expressing neurons (Figures 6E–6G). These findings suggest that INS-1::Venus is contained in synaptic or dense-core vesicles and transported to the presynaptic regions of the nerve ring processes.

INS-1 Insulin Acts in the AIA Interneurons

When *ins-1* was expressed in a subset of neurons including AIA neurons, using the *gpa-2* promoter or its

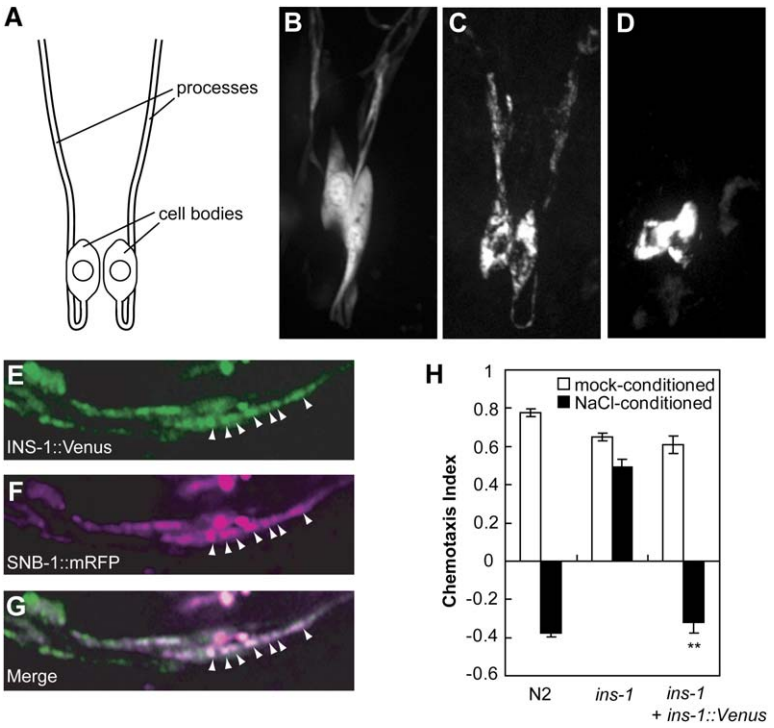

Figure 6. INS-1:Venus Is Localized to the Synaptic Regions of AIA Interneurons

(A) Schematic diagram of AIA interneurons. (B) Expression pattern of *Pins-1::Venus* in AIA interneurons. (C and D) Expression pattern of *Pins-1::ins-1::Venus* in AIA interneurons in wild-type N2 (C) and *unc-104(e1265)* (D) animals. In (B)–(D), stack images of various focal planes are merged. All panels show ventral view, anterior to the top. (E–G) Localization of INS-1::Venus and SNB-1::mRFP in the nerve ring processes of AIA interneurons. The lateral view of *unc-13(e51)* adult animals expressing *Pins-1::ins-1::Venus* (green) and *Pins-1::snb-1::mRFP* (magenda). *unc-13* mutants were used for better resolution of SNB-1::mRFP puncta (Chuang and Bargmann, 2005; Richmond et al., 1999). (H) INS-1::Venus rescues the learning defect of *ins-1(nr2091)* animals. Double asterisks represent significant differences from control *ins-1* animals carrying only the transformation marker (**p < 0.001 by Student's t test). Error bars represent SEM.

own promoter, the learning defect of *ins-1(nr2091)* mutants was almost completely rescued. In contrast, expression in chemosensory neurons or amphid interneurons other than AIA did not rescue the learning defect (Figure 7A). These results suggest that the expression of INS-1 in AIA neurons, or a subset of neurons including AIA, is sufficient for salt chemotaxis learning. If the expression of INS-1 in AIA neurons is required for the learning, animals lacking only AIA neurons should be defective in salt chemotaxis learning. To test this hypothesis, we performed salt learning assays with animals in which AIA neurons were killed by laser microsurgery. AIA-ablated animals were severely defective in salt chemotaxis learning (Figure 7B). In contrast, animals

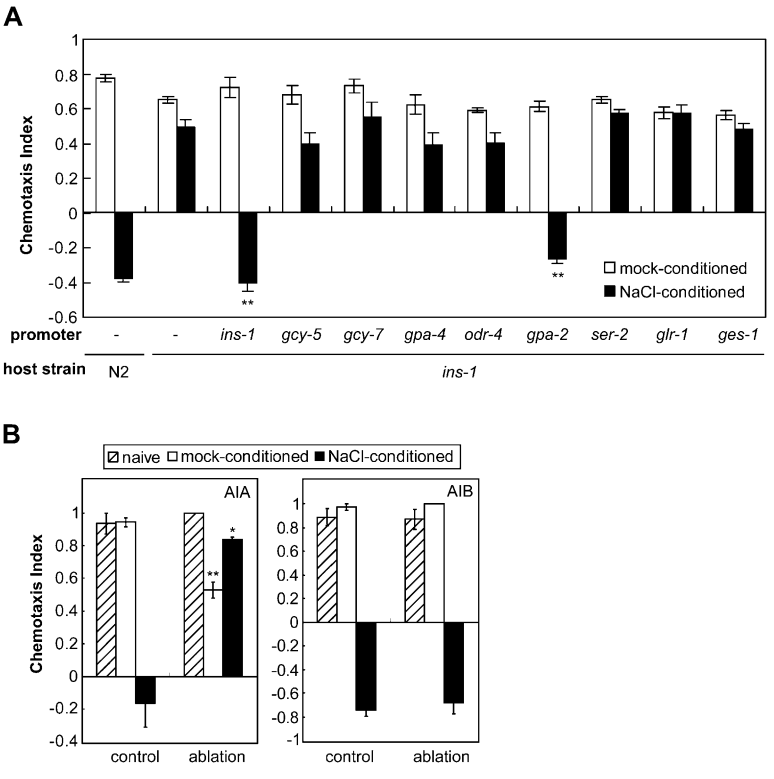

Figure 7. *ins-1* Acts in AIA Interneurons for Salt Chemotaxis Learning

(A) The learning defect of *ins-1(nr2091)* animals is rescued by the expression of *ins-1* in a subset of neurons including AIA interneurons using the *ins-1* or *gpa-2* promoter, but it is not rescued by the expression in ASER sensory neurons using the *gcy-5* promoter, in ASEL sensory neurons using the *gcy-7* promoter, in ASI sensory neurons using the *gpa-4* promoter, in all chemosensory neurons except for ASER/L using the *odr-4* promoter, a subset of neurons including AIY and AIZ interneurons using the *ser-2* promoter, a subset of neurons including AIB interneurons using the *glr-1* promoter, or intestine using the *ges-1* promoter. Double asterisks represent significant differences from control *ins-1* animals carrying only the transformation marker (**p < 0.001 by Student's t test). (B) AIA-ablated animals show a defect in salt chemotaxis learning (left), while AIB-ablated animals show normal salt chemotaxis learning (right). Asterisks represent significant differences from mock-ablated animals (*p < 0.01, **p < 0.001 by Student's t test). Error bars represent SEM.

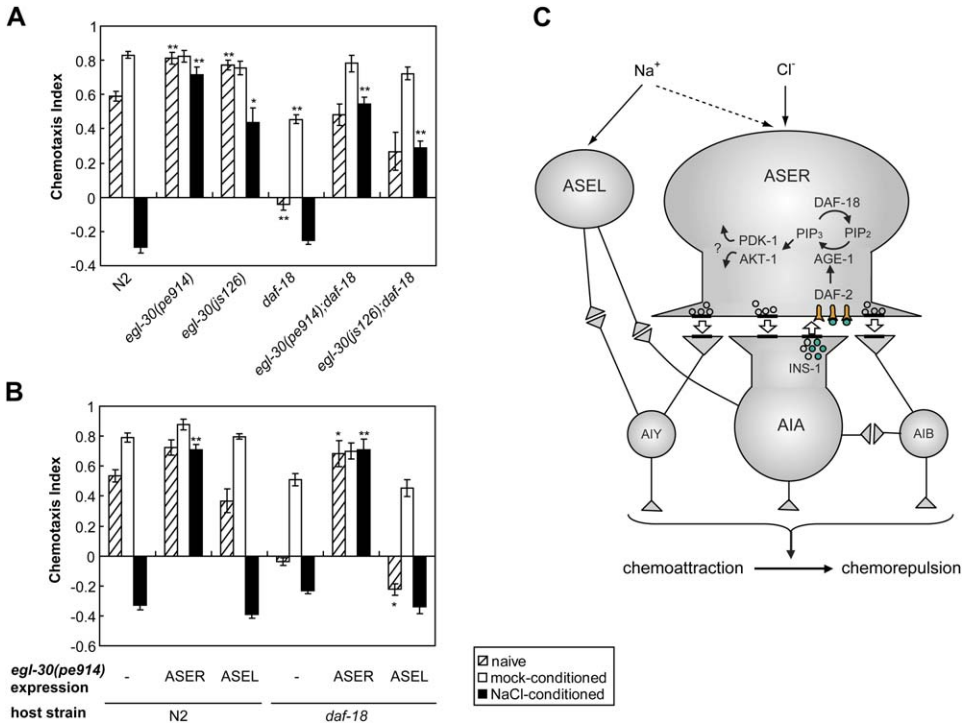

Figure 8. Chemotaxis Defect of the *daf-18* Mutant Is Suppressed by *egl-30* Mutations

(A) The learning assay was performed in wild-type N2 and *egl-30(pe914)*, *egl-30(js126)*, *daf-18(e1375)*, *egl-30(pe914); daf-18(e1375)*, and *egl-30(js126); daf-18(e1375)* mutant animals. Asterisks represent significant differences from wild-type N2 (*p < 0.01, **p < 0.001 by Student's t test).
(B) Expression of *egl-30(pe914)* in ASER neurons using the *gcy-5* promoter causes the learning defect in N2 animals and rescues the NaCl chemotaxis defect in *daf-18(e1375)* animals. On the other hand, expression in ASEL neurons using the *gcy-7* promoter has no effect on salt chemotaxis learning and NaCl chemotaxis in N2 and *daf-18(e1375)* animals, respectively. Asterisks represent significant differences from control animals carrying only the transformation marker (*p < 0.01 by Student's t test, **p < 0.001 by Student's t test).
(C) A model for the regulation of salt chemotaxis learning by the insulin-like signaling pathway. Insulin-like peptide INS-1 is secreted from AIA interneurons and activates insulin receptor DAF-2, PI 3-kinase AGE-1, and Ser/Thr kinases PDK-1 and AKT-1. The balance between this signaling and the activity of PTEN phosphatase DAF-18 regulates salt chemotaxis in the ASER neuron.
Error bars represent SEM.

without AIB neurons, which receive many synaptic outputs of AIA neurons, showed normal learning. These data indicate that AIA neurons, and presumably the secretion of INS-1 from these cells, are required for salt chemotaxis learning.

egl-30(gf) Suppresses the Chemotaxis Defect of *daf-18*

To identify candidates for factors acting downstream of the DAF-2/AGE-1 pathway, we mutagenized the *daf-18(e1375)* strain and screened for suppressor mutants with improved chemotaxis to salts (details will be published elsewhere). One of the suppressors obtained through this screening carried a point mutation, *pe914*, in the *egl-30* gene, which encodes the α subunit of the G protein G_q (Lackner et al., 1999). The previously reported gain-of-function mutation *egl-30(js126)* (Hawasli et al., 2004) also suppressed *daf-18(e1375)*. Both of these *egl-30* alleles, as single mutants, showed defects in salt chemotaxis learning (Figure 8A). Expression of *egl-30(pe914)* in ASER neurons was sufficient for the suppression of the chemotaxis defect in *daf-18(e1375)* animals and the induction of the learning defect in wild-type animals (Figure 8B). EGL-30 is known to positively regulate synaptic transmission in motor neurons (Lackner et al., 1999). These observations, therefore, suggest that the DAF-2/AGE-1 pathway may act by negatively regulating the synaptic outputs of the ASER sensory neuron.

Discussion

In this study, we obtained evidence that the insulin/PI 3-kinase pathway controls salt chemotaxis learning in *C. elegans*. Mutants of components of the insulin/PI 3-kinase pathway, *ins-1*, *daf-2*, *age-1*, *pdk-1*, and *akt-1*, showed defects in salt chemotaxis learning. The mutation of *daf-18*, which leads to an elevation of 3-phosphoinositides (Solari et al., 2005), caused a general reduction of salt chemotaxis, mimicking salt-conditioned states. Therefore, either raising or lowering the activity of the PI 3-kinase pathway directs changes in salt chemotaxis in opposite directions. In the total absence of the PI 3-kinase activity in *age-1(null); daf-18* mutants, only a small changes of chemotaxis was observed in salt chemotaxis learning. Therefore, the insulin/PI 3-kinase pathway appears to play a major role for the learning, although other signaling pathways also contribute to salt chemotaxis learning (Hukema et al., 2006; Ishihara et al., 2002).

Although recent evidence points to a role for PI 3-kinase in the generation of neuronal polarity and neurite extension (Adler et al., 2006; Chang et al., 2006; Shi et al., 2003), the behavioral defects we observed in the insulin/PI 3-kinase pathway mutants are unlikely to be caused by developmental defects for the following reasons. First, learning defects were observed when the temperature-sensitive *daf-2* mutants were grown at a permissive temperature and tested at a nonpermissive temperature. Second, the learning defect of *ins-1* mutants was rescued by the expression of *ins-1* at the adult stage. Third, the chemotaxis defect of *daf-18* was rescued by the expression of *daf-18* at the adult stage, and the transient overexpression of *daf-18* caused a learning defect. These observations, therefore, suggest that the insulin-like pathway regulates chemotaxis behavior and salt chemotaxis learning through active modulation of neural functions.

In our salt chemotaxis learning assay, chemotaxis of wild-type animals is increased after soaking in a NaCl-free buffer (mock conditioning) or incubation on a plate with fresh food (Figure 1B, Movies S1 and S3, and Figure S7A). In addition, salt chemotaxis of naive animals tends to show larger variability between experiments compared to mock-conditioned animals. We speculate that, during cultivation, worms might sense some sensory cue, which is functionally equivalent to partial starvation and could come from changing quality and quantity of bacterial food, and show some decrease in salt chemotaxis because standard cultivation plates contain 51 mM NaCl. Incubation in a NaCl-free buffer or fresh food might promote a recovery from these conditioned states. In *daf-2* mutants, chemotaxes of naive animals and animals incubated in a NaCl-free buffer or fresh food were not very different (Figures 1E and 2 and Figure S7B). This phenotype of *daf-2* mutants might be due to a defect in salt chemotaxis learning, although naive chemotaxis of *daf-2* mutants may be increased for other reasons, such as enhanced maintenance of neuronal functions, which were observed in various life-extending mutants (Murakami et al., 2005).

Functions of INS-1 and AIA Neurons in Salt Chemotaxis Learning

Our results of mutant phenotypes, cell-specific rescue experiments, and localization of INS-1 suggest that INS-1 is synthesized and secreted from AIA interneurons and acts on the ASER salt-sensing neuron to activate DAF-2 receptor, PI 3-kinase AGE-1, and downstream kinases PDK-1 and AKT-1 in ASER. Activated AKT-1 therefore appears to modulate the function of the ASER neuron (Figure 8C). INS-1::Venus was localized at the presynaptic region of AIA interneurons, and this localization was lost in *unc-104* KIF-1 mutants. Therefore, it seems likely that INS-1 acts as a neuropeptide, which acts through synaptic contacts, or a neurohormone, which acts more hormonally. It is interesting that AIA neurons that receive inputs from sensory neurons send the INS-1 signal back onto the sensory neuron ASER to modify its function. AIA neurons have reciprocal synapses with ASER at the contacts of AIA and ASER processes that run side by side in the nerve ring, but not with ASEL (White et al., 1986). If INS-1 acts through synaptic contacts, this synaptic organization could be the basis for the ASER-specific requirement for the DAF-2/AGE-1 pathway in salt chemotaxis learning. The feedback regulation by AIA neurons may be functionally similar to that by retinal amacrine cells and granule cells in the olfactory bulb or accessory olfactory bulb in mammals, all of which have dendro-dendritic reciprocal synapses with projection neurons that transmit sensory signals (Kaba et al., 1994; Vigh et al., 2005). A potential feedback regulation by neuropeptides was also reported in mechanosensory circuits in *C. elegans*; EGL-3, which encodes a homolog of proprotein convertase type 2 (PC2), acts at the command interneurons to regulate glutamatergic neurotransmission between ASH sensory neurons and the command interneurons in nose-touch response (Kass et al., 2001). A feedback inhibition by neuropeptides may be a general mechanism for modulation of animal behavior.

It was reported that, when INS-1 was overexpressed, it acted negatively on the DAF-2 pathway in the regulation of dauer formation (Pierce et al., 2001). However, overexpression of INS-1 had no effects on salt chemotaxis learning (data not shown), while the *ins-1* deletion mutant showed a defect similar to *daf-2* mutants, suggesting that INS-1 acts as an agonist of DAF-2. Therefore INS-1 may act in opposite directions for dauer formation and salt chemotaxis learning. The difference of recipient cell types and existence of unidentified cofactors or modifiers could lead to the difference in the responses between dauer formation and salt chemotaxis learning; the DAF-2 pathway acts in the ASER neuron for salt chemotaxis learning, while it acts in many cell types for dauer formation (Apfeld and Kenyon, 1998; Libina et al., 2003). Alternatively, constitutive overexpression of INS-1 may have caused downregulation of the receptor function in the previous report on dauer formation in a similar manner to hyperinsulinemia (Werner et al., 2004).

We do not know when and how INS-1 is secreted, but AIA receives direct synaptic inputs from ASE neurons and other amphid sensory neurons (White et al., 1986). Therefore, a possible scenario is that INS-1 is secreted from AIA upon excitation of these neurons during conditioning. One possibility is that INS-1 is secreted by starvation and stress signals, which are necessary for salt chemotaxis learning to occur. *ins-1(nr2091)* mutants also show defects in temperature learning (Ikue Mori, personal communication), in which worms learn to avoid cultivation temperature when raised in the absence of food (Mohri et al., 2005; Mori and Ohshima, 1995). On the other hand, *ins-1* mutants do not show obvious defects in the Hen assay (Takashi Murayama, Takeshi Ishihara, and Ikue Mori, personal communication), which tests the animals' abilities to balance the responses to a chemoattractant and a chemorepellent that are simultaneously presented (Ishihara et al., 2002). These observations are consistent with the view that *ins-1* may transmit the starvation signal.

However, other possibilities also remain. For example, INS-1 may be secreted constitutively to activate the DAF-2/AGE-1 pathway, and this signaling may be a prerequisite for other machinery to regulate salt chemotaxis learning. In this case, the insulin-like signaling pathway may act to maintain the property of the sensory neuron, such as the synaptic strength between the sensory neuron and interneurons, at an adequate level.

The Role of Sensory Neurons in the Behavioral Plasticity

The level of 3-phosphoinositides in ASER appears to determine the extent and orientation of chemotaxis to salts because cell-specific rescue experiments suggest that both AGE-1 and DAF-18 act in the ASER neuron (Figures 4A and 4B). It is interesting that the action of *age-1* in ASER alone can cause a change of chemotaxis from a positive to a negative orientation in salt-conditioned animals. Hukema et al. also reported the essential role of ASE neurons in a similar assay for plasticity of salt chemotaxis (Hukema et al., 2006). In addition, they suggested that other neurons, such as ASH, ASI, and ADF chemosensory neurons and sensory neurons exposed to the body fluid, are also required for the plasticity. These neurons might detect environmental signals, such as starvation, that are required for induction of plasticity of salt chemotaxis. Alternatively, they may mediate the salt-avoidance behavior seen in conditioned animals, possibly in an ASE-dependent manner.

How are the functions of ASE neurons modulated? Our MAPK and calcium-imaging data indicate that sensory response of the ASER neuron is not affected by the activity of DAF-2/AGE-1 pathway and therefore suggest that the pathway acts at the level of output of ASER neurons. Our genetic screen for mutants that suppress reduced chemotaxis of the *daf-18* mutant led us to obtain a mutant of *egl-30*. EGL-30 $G_q\alpha$ is known to regulate neurotransmitter release at the neuromuscular junction through production of presynaptic diacylglycerol (DAG), which facilitates neurotransmitter release (Lackner et al., 1999). These data imply that the DAF-2/AGE-1 signaling pathway might negatively regulate neurotransmitter release of the ASER neuron, thereby causing the dramatic reduction of salt chemotaxis, a hypothesis which should be tested by further molecular analyses of the pathway.

Are Roles for the Insulin/PI 3-Kinase Signaling Conserved?

In addition to regulation of energy metabolism in the peripheral tissues, insulin is believed to regulate learning and memory in the central nervous system in human and rodents. Insulin is known to be synthesized in the brain (Devaskar et al., 1994) and released under depolarizing conditions (Wei et al., 1990). Insulin receptors are expressed in several brain areas and are localized to synapses (Abbott et al., 1999). At the cellular level, insulin and/or PI 3-kinase regulate various processes: secretion of neuropeptides, activities and recycling of neurotransmitter receptors, activities of ion channels, and the response of olfactory neurons (Jonas et al., 1997; Man et al., 2003; Skeberdis et al., 2001; Spanswick et al., 2000; Spehr et al., 2002). From these observations, insulin may act as a neuromodulator in behavioral plasticity in mammals. However, the significance of these regulations is yet to be demonstrated. Because cellular and molecular mechanisms for the action of the insulin/PI 3-kinase signaling pathway may be conserved among a wide range of genera (Wu et al., 2005), further understanding of the regulation of neural functions by the insulin/PI 3-kinase pathway may be facilitated by using the model system provided in this report.

Experimental Procedures

Strains and Culture

C. elegans strains were cultivated at 15°C or 20°C under standard conditions (Brenner, 1974), except that the *E. coli* strain NA22 was used as a food source. Strains used were wild-type Bristol N2, *daf-16(m26)*, *daf-16(mgDf47)* I , *unc-13(e51)* I, *egl-30(js126)*, *egl-30(pe914)* I, *age-1(hx546)*, *age-1(mg305)*, *age-1(m333)* II, *unc-104(e1265)* II, *daf-2(sa189)*, *daf-2(sa219)*, *daf-2(e1370)*, *daf-2(m41)* III, *ins-1(nr2091)* IV, *daf-18(e1375)*, *daf-18(mg198)* IV, *daf-28(sa191)* V, *akt-1(ok525)* V, *pdk-1(sa680)* X, *gpc-1(pk298)* X, *hen-1(tm501)* X, *adp-1(ky20)*, and *ntIs1* (*Pgcy-5::gfp*). The temperature-sensitive allele of *age-1*, *mg305*, was a generous gift from Patrick Hu and Gary Ruvkun.

Salt Chemotaxis Learning Assay

The chemotaxis assay was performed using a 9 cm assay plate (5 mM KPO_4, pH 6.0, 1 mM $CaCl_2$, 1 mM $MgSO_4$, 2% agar), on which a salt gradient had been formed overnight by placing an agar plug containing 100 mM of NaCl (5 mm diameter) close to the edge of the plate. One microliter each of 0.5 M sodium azide was spotted at the gradient peak and at the opposite ends of the plates, just before placing the animals. In the experiments shown in Figure 7B, a 6 cm assay plate (5 mM KPO_4, pH 6.0, 1 mM $CaCl_2$, 1 mM $MgSO_4$, 2% agar) was used, on which a salt gradient had been formed using an agar plug containing 50 mM NaCl. For learning assays, young adults grown on NGM plates seeded with *E. coli* NA22 were collected, washed, transferred to a conditioning buffer (5 mM KPO_4, pH 6.0, 1 mM $CaCl_2$, 1 mM $MgSO_4$) with 20 mM NaCl (NaCl conditioning) or without NaCl (mock conditioning), and incubated at 25°C for 1 hr. After the incubation, animals were directly placed at the center of the assay plates, and then incubated at 25°C for 30 min., except in Figure 7B, where the incubation time was 15 min. The chemotaxis index was calculated as $(A - B)/(N - C)$ where A was the number of animals within 2 cm of the peak of the salt gradient, B was the number of animals within 2 cm of the control spot, N was the number of all animals on an assay plate, and C was the number of animals that did not move in the central region (see diagram of the assay plate in Figure S8). One hundred to two hundred animals were used in each assay, and assays were performed at least four times in each experiment except for the experiments using cell-ablated animals (see Supplemental Experimental Procedures).

MAP Kinase Immunostaining

ntIs1 (chromosomally integrated *Pgcy-5::gfp*) animals, which express GFP in ASER neurons, were synchronized by bleaching followed by overnight incubation in M9 buffer and incubated at either 15°C (for *daf-2* mutants) or 20°C (all other strains). When grown to the L4 stage, animals were collected from the culture plates with wash buffer (5 mM KPO_4, pH 6.0, 1 mM $CaCl_2$, 1 mM $MgSO_4$, 0.05% gelatin) (upshift) or wash buffer with 50 mM NaCl (downshift) and washed twice by centrifugation at 3000 rpm with the same buffer and kept at the room temperature (23°C). At 10 min after the harvest, animals were then transferred to either wash buffer with 50 mM NaCl (upshift) or wash buffer (downshift) and collected and fixed at intervals. Similar responses to downshift were observed when animals were kept for 60 min in 50 mM NaCl before downshift or when animals were directly washed from culture plates (which contain 51 mM NaCl) into NaCl-free wash buffer (data not shown). Fixation and immunostaining were performed as previously described (Hirotsu et al., 2000) except that anti-diphosphorylated (activated) MAPK antibody (Sigma) was used at a 1:100 dilution and anti-GFP antibody (Santa Cruz) was used at a 1:800 dilution. The fraction of animals in which the GFP-positive cell (ASER neuron) was also stained for anti-activated-MAPK was counted. A total of at least 100 animals was counted for each time point. Scoring was made by an experimenter who was unaware of the identity of the samples.

In Vivo Calcium Imaging from ASER

Sample preparation, delivery of stimulant, optical recordings, and image analysis were performed as described with some modifications (Hilliard et al., 2005; Kerr et al., 2000). *flp-6::YC2.12* strains expressing YC2.12 in ASE sensory neurons were glued on agarose pads and covered with saline containing 40 mM NaCl under microscope. The worms were exposed to a constant flow of 40 mM

NaCl-saline for ~20 min before imaging for conditioning. To apply 40–0 mM NaCl downstep stimulation, a stream of stimulant saline containing 0 mM NaCl was guided through capillary to cover the worm's head (Hilliard et al., 2005). Both saline solutions were adjusted at 350 mOsm by glycerol. ASER images in YFP and CFP channels were simultaneously captured at 10 Hz by using a Hamamatsu Orca ER CCD camera and a Hamamatsu W-View emission image splitter. The image capturing and analysis was performed as described before (Hilliard et al., 2005). Ratio changes were parameterized using scripts for MATLAB (The Mathworks), and the magnitude was compared for wild-type N2, *daf-18(mg198*null*)*, and *age-1(hx546rf)* by using a modified Mann-Whitney rank statistics test.

See Supplemental Experimental Procedures for determination of recovery time course (Figure 1D), plasmid construction, germline transformation, cell ablation, heat-shock experiments, and salt chemotaxis learning assay for Figures S1 and S2.

Supplemental Data

The Supplemental Data for this article can be found online at http://www.neuron.org/cgi/content/full/51/5/613/DC1/.

Acknowledgments

We specially thank G. Ruvkun and Patrick Hu for the *ins-1(nr2091)*, *age-1(mg305)*, and *daf-18(mg198)* strains; C.A. Wolkow for the *age-1* cDNA; and K. Kimura for the *daf-2* cDNA and detailed information on *daf-2* rescue experiments. We also thank Y. Kohara for the *daf-18* cDNA; M. Doi for the *egl-30* cDNA; T. Hirotsu for the *snb-1*::DsRed clone; Y. Oshima and K. Ogura for the *unc-14* promoter; O. Hobert for the *ttx-3* promoter; R. Tsien for mRFP; A. Fire for vectors; *C. elegans* Knockout Consortium for the *akt-1(ok525)* strain; T. Tanaka for experimental assistance; T. Murayama, T. Ishihara, and I. Mori for communicating unpublished results and for discussion; and I. Katsura for comments on the manuscript. All other nematode strains used in this study were provided by the Caenorhabditis Genetics Center (CGC), which is funded by the NIH National Center for Research Resources (NCRR). This work was supported in part from grants from NIDA and the Human Frontier Science Program (to W.R.S.) and Grant-in-Aid for Scientific Research from the Ministry of Education, Culture, Sports, Science and Technology of Japan (to Y.I.).

Received: February 27, 2006
Revised: June 23, 2006
Accepted: July 24, 2006
Published: September 6, 2006

References

Abbott, M.A., Wells, D.G., and Fallon, J.R. (1999). The insulin receptor tyrosine kinase substrate p58/53 and the insulin receptor are components of CNS synapses. J. Neurosci. *19*, 7300–7308.

Adler, C.E., Fetter, R.D., and Bargmann, C.I. (2006). UNC-6/Netrin induces neuronal asymmetry and defines the site of axon formation. Nat. Neurosci. *9*, 511–518.

Apfeld, J., and Kenyon, C. (1998). Cell nonautonomy of *C. elegans daf-2* function in the regulation of diapause and life span. Cell *95*, 199–210.

Bargmann, C.I., and Mori, I. (1997). Chemotaxis and thermotaxis. In C. elegans II, D.L. Riddle, T. Blumenthal, B.J. Meyer, and J.R. Priess, eds. (Cold Spring Harbor, NY: Cold Spring Harbor Laboratory Press), pp. 717–738.

Brenner, S. (1974). The genetics of *Caenorhabditis elegans*. Genetics *77*, 71–94.

Chang, S., Johnston, R.J., Jr., and Hobert, O. (2003). A transcriptional regulatory cascade that controls left/right asymmetry in chemosensory neurons of *C. elegans*. Genes Dev. *17*, 2123–2137.

Chang, C., Adler, C.E., Krause, M., Clark, S.G., Gertler, F.B., Tessier-Lavigne, M., and Bargmann, C.I. (2006). MIG-10/lamellipodin and AGE-1/PI3K promote axon guidance and outgrowth in response to slit and netrin. Curr. Biol. *16*, 854–862.

Chuang, C.F., and Bargmann, C.I. (2005). A Toll-interleukin 1 repeat protein at the synapse specifies asymmetric odorant receptor expression via ASK1 MAPKKK signaling. Genes Dev. *19*, 270–281.

Colbert, H.A., and Bargmann, C.I. (1995). Odorant-specific adaptation pathways generate olfactory plasticity in *C. elegans*. Neuron *14*, 803–812.

Colbert, H.A., Smith, T.L., and Bargmann, C.I. (1997). OSM-9, a novel protein with structural similarity to channels, is required for olfaction, mechanosensation, and olfactory adaptation in *Caenorhabditis elegans*. J. Neurosci. *17*, 8259–8269.

Devaskar, S.U., Giddings, S.J., Rajakumar, P.A., Carnaghi, L.R., Menon, R.K., and Zahm, D.S. (1994). Insulin gene expression and insulin synthesis in mammalian neuronal cells. J. Biol. Chem. *269*, 8445–8454.

Faumont, S., Miller, A.C., and Lockery, S.R. (2005). Chemosensory behavior of semi-restrained *Caenorhabditis elegans*. J. Neurobiol. *65*, 171–178.

Hawasli, A.H., Saifee, O., Liu, C., Nonet, M.L., and Crowder, C.M. (2004). Resistance to volatile anesthetics by mutations enhancing excitatory neurotransmitter release in *Caenorhabditis elegans*. Genetics *168*, 831–843.

Hilliard, M.A., Apicella, A.J., Kerr, R., Suzuki, H., Bazzicalupo, P., and Schafer, W.R. (2005). In vivo imaging of *C. elegans* ASH neurons: cellular response and adaptation to chemical repellents. EMBO J. *24*, 63–72.

Hirotsu, T., Saeki, S., Yamamoto, M., and Iino, Y. (2000). The Ras-MAPK pathway is important for olfaction in *Caenorhabditis elegans*. Nature *404*, 289–293.

Hobert, O. (2003). Behavioral plasticity in *C. elegans*: paradigms, circuits, genes. J. Neurobiol. *54*, 203–223.

Hukema, R.K., Rademakers, S., Dekkers, M.P., Burghoorn, J., and Jansen, G. (2006). Antagonistic sensory cues generate gustatory plasticity in *Caenorhabditis elegans*. EMBO J. *25*, 312–322.

Ishihara, T., Iino, Y., Mohri, A., Mori, I., Gengyo-Ando, K., Mitani, S., and Katsura, I. (2002). HEN-1, a secretory protein with an LDL receptor motif, regulates sensory integration and learning in *Caenorhabditis elegans*. Cell *109*, 639–649.

Jansen, G., Weinkove, D., and Plasterk, R.H. (2002). The G-protein gamma subunit *gpc-1* of the nematode *C.elegans* is involved in taste adaptation. EMBO J. *21*, 986–994.

Jonas, E.A., Knox, R.J., Smith, T.C., Wayne, N.L., Connor, J.A., and Kaczmarek, L.K. (1997). Regulation by insulin of a unique neuronal Ca^{2+} pool and of neuropeptide secretion. Nature *385*, 343–346.

Kaba, H., Hayashi, Y., Higuchi, T., and Nakanishi, S. (1994). Induction of an olfactory memory by the activation of a metabotropic glutamate receptor. Science *265*, 262–264.

Kass, J., Jacob, T.C., Kim, P., and Kaplan, J.M. (2001). The EGL-3 proprotein convertase regulates mechanosensory responses of *Caenorhabditis elegans*. J. Neurosci. *21*, 9265–9272.

Kerr, R., Lev-Ram, V., Baird, G., Vincent, P., Tsien, R.Y., and Schafer, W.R. (2000). Optical imaging of calcium transients in neurons and pharyngeal muscle of *C. elegans*. Neuron *26*, 583–594.

Kimura, K.D., Tissenbaum, H.A., Liu, Y., and Ruvkun, G. (1997). *daf-2*, an insulin receptor-like gene that regulates longevity and diapause in *Caenorhabditis elegans*. Science *277*, 942–946.

L'Etoile, N.D., Coburn, C.M., Eastham, J., Kistler, A., Gallegos, G., and Bargmann, C.I. (2002). The cyclic GMP-dependent protein kinase EGL-4 regulates olfactory adaptation in *C. elegans*. Neuron *36*, 1079–1089.

Lackner, M.R., Nurrish, S.J., and Kaplan, J.M. (1999). Facilitation of synaptic transmission by EGL-30 Gqalpha and EGL-8 PLCbeta: DAG binding to UNC-13 is required to stimulate acetylcholine release. Neuron *24*, 335–346.

Li, W., Kennedy, S.G., and Ruvkun, G. (2003). *daf-28* encodes a *C. elegans* insulin superfamily member that is regulated by environmental cues and acts in the DAF-2 signaling pathway. Genes Dev. *17*, 844–858.

Libina, N., Berman, J.R., and Kenyon, C. (2003). Tissue-specific activities of *C. elegans* DAF-16 in the regulation of lifespan. Cell *115*, 489–502.

Lin, C.H., Yeh, S.H., Lu, K.T., Leu, T.H., Chang, W.C., and Gean, P.W. (2001). A role for the PI-3 kinase signaling pathway in fear conditioning and synaptic plasticity in the amygdala. Neuron *31*, 841–851.

Man, H.Y., Lin, J.W., Ju, W.H., Ahmadian, G., Liu, L., Becker, L.E., Sheng, M., and Wang, Y.T. (2000). Regulation of AMPA receptor-mediated synaptic transmission by clathrin-dependent receptor internalization. Neuron *25*, 649–662.

Man, H.Y., Wang, Q., Lu, W.Y., Ju, W., Ahmadian, G., Liu, L., D'Souza, S., Wong, T.P., Taghibiglou, C., Lu, J., et al. (2003). Activation of PI3-kinase is required for AMPA receptor insertion during LTP of mEPSCs in cultured hippocampal neurons. Neuron *38*, 611–624.

Miller, A.C., Thiele, T.R., Faumont, S., Moravec, M.L., and Lockery, S.R. (2005). Step-response analysis of chemotaxis in *Caenorhabditis elegans*. J. Neurosci. *25*, 3369–3378.

Mori, I., and Ohshima, Y. (1995). Neural regulation of thermotaxis in *Caenorhabditis elegans*. Nature *376*, 344–348.

Mohri, A., Kodama, E., Kimura, K.D., Koike, M., Mizuno, T., and Mori, I. (2005). Genetic control of temperature preference in the nematode *Caenorhabditis elegans*. Genetics *169*, 1437–1450.

Murakami, H., Bessinger, K., Hellmann, J., and Murakami, S. (2005). Aging-dependent and -independent modulation of associative learning behavior by insulin/insulin-like growth factor-1 signal in *Caenorhabditis elegans*. J. Neurosci. *25*, 10894–10904.

Nagai, T., Ibata, K., Park, E.S., Kubota, M., Mikoshiba, K., and Miyawaki, A. (2002). A variant of yellow fluorescent protein with fast and efficient maturation for cell-biological applications. Nat. Biotechnol. *20*, 87–90.

Nonet, M.L., Saifee, O., Zhao, H., Rand, J.B., and Wei, L. (1998). Synaptic transmission deficits in *Caenorhabditis elegans* synaptobrevin mutants. J. Neurosci. *18*, 70–80.

Paradis, S., Ailion, M., Toker, A., Thomas, J.H., and Ruvkun, G. (1999). A PDK1 homolog is necessary and sufficient to transduce AGE-1 PI3 kinase signals that regulate diapause in *Caenorhabditis elegans*. Genes Dev. *13*, 1438–1452.

Pierce, S.B., Costa, M., Wisotzkey, R., Devadhar, S., Homburger, S.A., Buchman, A.R., Ferguson, K.C., Heller, J., Platt, D.M., Pasquinelli, A.A., et al. (2001). Regulation of DAF-2 receptor signaling by human insulin and *ins-1*, a member of the unusually large and diverse *C. elegans* insulin gene family. Genes Dev. *15*, 672–686.

Pierce-Shimomura, J.T., Faumont, S., Gaston, M.R., Pearson, B.J., and Lockery, S.R. (2001). The homeobox gene *lim-6* is required for distinct chemosensory representations in *C. elegans*. Nature *410*, 694–698.

Richmond, J.E., Davis, W.S., and Jorgensen, E.M. (1999). UNC-13 is required for synaptic vesicle fusion in *C. elegans*. Nat. Neurosci. *2*, 959–964.

Riddle, D.L., and Albert, P.S. (1997). Genetic and environmental regulation of Dauer larva development. In C. elegans II, D.L. Riddle, T. Blumenthal, B.J. Meyer, and J.R. Priess, eds. (Cold Spring Harbor, NY: Cold Spring Harbor Laboratory Press), pp. 739–768.

Saeki, S., Yamamoto, M., and Iino, Y. (2001). Plasticity of chemotaxis revealed by paired presentation of a chemoattractant and starvation in the nematode *Caenorhabditis elegans*. J. Exp. Biol. *204*, 1757–1764.

Scott, B.A., Avidan, M.S., and Crowder, C.M. (2002). Regulation of hypoxic death in *C. elegans* by the insulin/IGF receptor homolog DAF-2. Science *296*, 2388–2391.

Shi, S.H., Jan, L.Y., and Jan, Y.N. (2003). Hippocampal neuronal polarity specified by spatially localized mPar3/mPar6 and PI 3-kinase activity. Cell *112*, 63–75.

Skeberdis, V.A., Lan, J., Zheng, X., Zukin, R.S., and Bennett, M.V. (2001). Insulin promotes rapid delivery of N-methyl-D- aspartate receptors to the cell surface by exocytosis. Proc. Natl. Acad. Sci. USA *98*, 3561–3566.

Solari, F., Bourbon-Piffaut, A., Masse, I., Payrastre, B., Chan, A.M., and Billaud, M. (2005). The human tumour suppressor PTEN regulates longevity and dauer formation in *Caenorhabditis elegans*. Oncogene *24*, 20–27.

Spanswick, D., Smith, M.A., Mirshamsi, S., Routh, V.H., and Ashford, M.L. (2000). Insulin activates ATP-sensitive K^+ channels in hypothalamic neurons of lean, but not obese rats. Nat. Neurosci. *3*, 757–758.

Spehr, M., Wetzel, C.H., Hatt, H., and Ache, B.W. (2002). 3-phosphoinositides modulate cyclic nucleotide signaling in olfactory receptor neurons. Neuron *33*, 731–739.

Suzuki, H., Kerr, R., Bianchi, L., Frokjaer-Jensen, C., Slone, D., Xue, J., Gerstbrein, B., Driscoll, M., and Schafer, W.R. (2003). In vivo imaging of *C. elegans* mechanosensory neurons demonstrates a specific role for the MEC-4 channel in the process of gentle touch sensation. Neuron *39*, 1005–1017.

Vigh, J., Li, G.L., Hull, C., and von Gersdorff, H. (2005). Long-Term plasticity mediated by mGluR1 at a retinal reciprocal synapse. Neuron *46*, 469–482.

Wei, L.T., Matsumoto, H., and Rhoads, D.E. (1990). Release of immunoreactive insulin from rat brain synaptosomes under depolarizing conditions. J. Neurochem. *54*, 1661–1665.

Werner, E.D., Lee, J., Hansen, L., Yuan, M., and Shoelson, S.E. (2004). Insulin resistance due to phosphorylation of insulin receptor substrate-1 at serine 302. J. Biol. Chem. *279*, 35298–35305.

White, J.G., Southgate, E., Thomson, J.N., and Brenner, S. (1986). The structure of the nervous system of *Caenorhabditis elegans*. Philos. Trans. R. Soc. Lond. B Biol. Sci. *314*, 1–340.

Wu, Q., Zhao, Z., and Shen, P. (2005). Regulation of aversion to noxious food by Drosophila neuropeptide Y- and insulin-like systems. Nat. Neurosci. *8*, 1350–1355.

Zahn, T.R., Angleson, J.K., MacMorris, M.A., Domke, E., Hutton, J.F., Schwartz, C., and Hutton, J.C. (2004). Dense core vesicle dynamics in *Caenorhabditis elegans* neurons and the role of kinesin UNC-104. Traffic *5*, 544–559.

Zhao, W.Q., Chen, H., Quon, M.J., and Alkon, D.L. (2004). Insulin and the insulin receptor in experimental models of learning and memory. Eur. J. Pharmacol. *490*, 71–81.